Atmos. Chem. Phys. Discuss., 11, 26741–26789, 2011
www.atmos-chem-phys-discuss.net/11/26741/2011/
doi:10.5194/acpd-11-26741-2011

Atmospheric Chemistry and Physics Discussions

The scale problem in quantifying aerosol indirect effects

A. McComiskey[1,2] **and G. Feingold**[2]

[1]Cooperative Institute for Research in Environmental Sciences, University of Colorado, Boulder, USA
[2]NOAA Earth System Research Laboratory Chemical Sciences Division, 325 Broadway Boulder, CO 80305, USA

Received: 10 September 2011 – Accepted: 14 September 2011 – Published: 27 September 2011

Correspondence to: A. McComiskey (allison.mccomiskey@noaa.gov)

Published by Copernicus Publications on behalf of the European Geosciences Union.

Abstract

A wide range of estimates exists for the radiative forcing of the aerosol effect on cloud albedo. We argue that a component of this uncertainty derives from the use of a wide range of observational scales and platforms. Aerosol affects cloud properties at the microphysical scale, or the “process scale” but observations are most often made of bulk properties over a wide range of resolutions, or “analysis scales”. We show that differences between process and analysis scales incur biases in quantification of the albedo effect through the impact that data aggregation has on statistical properties of the aerosol or cloud variable, and their covariance. Measures made within this range of scales are erroneously treated as equivalent, leading to a large uncertainty in associated radiative forcing estimates. Issues associated with the coarsening of observational resolution particular to quantifying the albedo effect are discussed. Specifically, the omission of the constraint on cloud liquid water path and the separation in space of cloud and aerosol properties from passive, space-based remote sensors dampen the measured strength of the albedo effect. Based on our understanding of these biases we propose a new approach for an observationally-based, robust method for estimating aerosol indirect effects that can be used for radiative forcing estimates as well as a better characterization of the uncertainties associated with those estimates.

1 Introduction

Boundary layer clouds have been identified as a major source of uncertainty in climate sensitivity and climate change (Bony and Dufresne, 2006; Medeiros et al., 2008). The influence of aerosol particles on these clouds, via modification to microphysical processes, further contributes to this uncertainty. Aerosol has potentially substantial impacts on cloud radiative forcing (“aerosol indirect effects”), cloud-climate feedbacks, and water resources through changing patterns of precipitation; however, quantifying

ACPD
11, 26741–26789, 2011

the associated mechanisms and impacts through observation, and representing those processes in models, has proven to be extremely challenging.

Of several defined indirect effects, only the first aerosol indirect effect, or albedo effect (Twomey, 1974), has been considered a radiative forcing, rather than a feedback, and therefore included in the Intergovernmental Panel on Climate Change (Forster, 2007) radiative forcing estimates. The sign of its forcing is agreed to be negative but there is a wide range in the estimated magnitude. This IPCC estimate comprises results from general, circulation models (GCM) and includes no estimates from observations alone. A few studies have produced purely observationally based estimates of the first indirect effect radiative forcing (e.g. Quaas et al., 2008; Lebsock et al., 2008) and inverse calculations based on observations have also been performed (e.g. Murphy et al., 2009). These tend to be at the low end of the range produced by GCMs. Other indirect effects related to cloud water variability and precipitation that potentially affect cloud amount and lifetime, are considered feedbacks, and have a poorly quantified impact on the radiation budget (Quaas et al., 2009; Lohmann et al., 2010). The numerous studies that have attempted to assess the magnitude of these effects have generated conflicting answers, and even the sign of the cloud water response to changes in the aerosol is in question (Albrecht, 1989; Ackerman et al., 2004; Brenguier et al., 2003; Matsui et al., 2006; Xue et al., 2008; Lebsock et al., 2008).

Regardless of the somewhat arbitrary distinction between the “forcing” and “feedback” nature of aerosol-cloud interactions, we argue that important observational aspects of aerosol-cloud interactions have not been adequately addressed. First, obtaining direct, independent, and collocated measurements of each pertinent variable is difficult. Further, there is a range of observational scales or “analysis scales” to consider that are usually different from the scale of the driving mechanism or “process scale”. The most accurate representation of a process results from an analysis in which the process scale and analysis scale are the same. Scale is a quality intrinsic to every property and process, and yet, as this examination of aerosol-cloud interactions will show, has not been fully considered in current observational efforts. Current

ACPD
11, 26741–26789, 2011

analyses of the cloud-albedo effect span scales from the microphysical to the global (see references in Table 1). This spectrum of analyses has grown out of an interest to link important microphysical processes with the resulting radiative impacts at larger, climatically relevant scales. Without discounting the potential importance of microphysical processes resulting in emergent properties at larger-scales, the scales of interest for radiative forcing (meso-to-global scale) are different from the microphysical scale at which the driving processes operate. Using the same methodology for quantifying aerosol-cloud interactions with inputs at different scales produces results that are not equivalent to each other and care must be taken in their interpretation. The physical meaning of typical quantified values found in the literature from this spectrum of scales has, thus far, not been characterized. It is our assertion that disparities in scale among various physical processes, inconsistencies in scale among observations from various platforms, and disparities in the scales of representations (parameterizations) in models is responsible for a large part of the confusion in estimating the magnitude of indirect effects. This paper explores the impact of scale on quantifying aerosol-cloud interactions and their radiative forcings, and considers options for more accurate and relevant observational radiative forcing estimates.

2 Aggregation and scale biases in statistics

2.1 Current state of understanding aerosol-cloud interactions

Among the aerosol indirect effects, the IPCC estimates the radiative forcing of the first indirect effect, or albedo effect (Twomey, 1974) only. This quantity has the largest uncertainty of all of the radiative forcings and is also the only estimate derived solely from model results. A breakdown of the radiative forcing estimates by each of the IPCC Fourth Assessment Report (AR4) models is shown in Fig. 1a. The closed circles indicate models that represent the cloud-albedo effect through the use of drop activation parameterizations and the open circles indicate models that use satellite-based

ACPD
11, 26741–26789, 2011

empirical parameterizations. The models that apply empirical relationships between cloud and aerosol properties consistently predict the weakest radiative forcing. The latter are similar in magnitude to the purely satellite-based assessments such as those reported e.g. by Quaas et al. (2008), although these estimates are not included in AR4.

Empirical estimates of aerosol-cloud interactions derive from a range of in situ airborne measurements, ground-based remote sensing, and space-based remote sensing of aerosol and cloud properties. Twomey (1974) used airborne, process-scale measurements to show that an increase in cloud condensation nuclei from pollution would result in brighter clouds by increasing cloud optical depth, all else being equal. This approach required the cloud water variable be constrained in order to assess the impact of the aerosol on cloud albedo while controlling for other impacts on the cloud albedo. To quantify the microphysical component of the albedo effect, Feingold et al. (2001) proposed a metric $\mathrm{IE} = -d \ln r_\mathrm{e}/d \ln \tau_\mathrm{a}$, where r_e is the cloud drop effective radius and τ_a, the aerosol optical depth and holding cloud liquid water constant for all calculations. Later, the terminology for this calculation was changed to ACI (aerosol-cloud interactions) to clarify that the result represents not the indirect effect, which is a response of cloud albedo to aerosol, but instead the microphysical response of the albedo effect (McComiskey et al., 2009). Several other terminologies have been used in the literature, but for consistency ACI will be used throughout this work.

ACI has been reported or derived from measurements published in the literature for almost two decades. A variety of proxies has been used to represent the aerosol particles affecting the cloud, including aerosol number concentration N_a, aerosol optical depth τ_a, and aerosol index (AI) (the product of τ_a and the Ångstrom exponent), all of which will henceforth be denoted by α. Similarly, various proxies have been used to represent the cloud response to the change in aerosol, e.g. cloud optical depth τ_c, cloud drop number concentration N_d, and r_e. Using data for which the analysis scale closely matched the process scale, McComiskey et al. (2009) showed empirically that there is consistency amongst calculations of ACI using different microphysical proxies, provided the appropriate constraint on cloud liquid water path L is applied. Thus,

ACPD
11, 26741–26789, 2011

A. McComiskey and G. Feingold

$$\mathrm{ACI}_\tau = \frac{\partial \ln \tau_\mathrm{c}}{\partial \ln \alpha} \qquad 0 < \mathrm{ACI}_\tau < 0.33 \tag{1a}$$

$$\mathrm{ACI}_\mathrm{r} = -\frac{\partial \ln r_\mathrm{e}}{\partial \ln \alpha} \qquad 0 < \mathrm{ACI}_\tau < 0.33 \tag{1b}$$

$$\mathrm{ACI}_N = -\frac{d \ln N_\mathrm{d}}{d \ln \alpha} \qquad 0 < \mathrm{ACN}_N 1 \tag{1c}$$

$$\mathrm{ACI}_\tau = -\mathrm{ACI}_r = 1/3\mathrm{ACI}_\mathrm{N}. \tag{1d}$$

Figure 1b presents a representative selection of ACI_τ values ($0 \leq \mathrm{ACI} \leq 0.33$) from the literature originating from a range of observational platforms. Closed symbols denote studies where calculations were constrained by L and open symbols denote studies for which this constraint was ignored. It is clear that quantification of the albedo effect is sensitive to scale and to the constraint on L. The studies that occupy the coarsest resolutions on this plot were intentionally undertaken at resolutions that are comparable to GCM grid cell sizes in order to produce evaluation datasets or empirical parameterizations for those models. The association between weak radiative forcing and these coarse-scale parameterizations as opposed to stronger radiative forcing from both microphysical scale observations and model schemes becomes evident.

Published ACI values span almost the entire physically meaningful range from 0 to 0.33 (see Table 1). Data types used as input to these calculations range from those in which the process and analysis scales are closely matched to those in which the analysis scales are highly aggregated relative to the process scale. This begs the question: to what extent are these values meaningful and useful?

Observational estimates of the albedo effect have been omitted in the overall radiative forcing estimate of the albedo effect in the IPCC AR4, so we perform rough calculations based on ACI. At the right of Fig. 1a, the overall IPCC radiative forcing

ACPD
11, 26741–26789, 2011

(grey bar with range) is compared to a rough, 1-D (plane-parallel) calculation of what the range of forcing for the observations in Fig. 1b would be, following radiative transfer calculations in McComiskey and Feingold (2008). The calculations assume a factor of 3 increase in cloud condensation nucleus concentrations N_{CCN} and a global average liquid water cloud cover of 25 % with mean $L = 125\,\mathrm{g\,m^{-2}}$. ACI is varied over nearly the entire range of observed values from Fig. 1b. The result is a range in forcing from −0.2 to $-3.9\,\mathrm{W\,m^{-2}}$, much larger than the range estimated from GCMs. Figure 2 shows the variability in forcing as a function of ACI for various L and (CCN) perturbations for 1-D or plane-parallel conditions (100 % cloud cover). While this is a rudimentary estimate of the range of radiative forcing from observations with broad assumptions, it illustrates that observationally-based radiative forcing estimates of this kind are too variable to be useful.

If uncertainties in radiative forcing of aerosol indirect effects are to be reduced, it is necessary to understand what drives the scale biases seen in Fig. 1, both in how they relate to quantifying the albedo effect, and also in how they may bias analyses of all indirect effects including, for example, the impact of aerosol on cloud cover or precipitation. In the following sections, we attempt to define the factors contributing to these biases and provide some potential solutions that allow for a useable observationally based estimate as well as a more useful empirical parameterization or evaluation dataset for models.

2.2 Scale and statistics

The concept of "ecological fallacy" gained much attention in that field when Robinson (1950) illustrated that inferring characteristics of relationships among individuals from area-aggregated units did not produce reliable results. Since then, the difficulty in producing reliable statistics from aggregated areal data has been a subject of much concern in fields such as ecology and geography. We will borrow from the field of geography, where the Modifiable Areal Unit Problem (MAUP) (Openshaw, 1984) has

ACPD
11, 26741–26789, 2011

been used to describe the effect of level of aggregation (the scale problem) on uni- and multi-variate statistics.

It has long been understood that aggregation of data causes biases and error in statistical inferences through its smoothing effect on the data. Signals that occur at scales smaller than the analysis scale will be lost at coarser resolutions. This effect can be visualized very simply using the examples in Fig. 3. The top row provides a simple and contrived example (from Jelinski and Wu, 1996) for which the variance s^2 goes to zero with increased aggregation. The bottom row presents randomly generated numbers between 0 and 1 for which the variance is substantially diminished with aggregation. Note that for aggregation that involves direct averaging of adjacent cells on a regular grid the mean μ is unaffected.

The ensuing effects of aggregation and loss of variance on common calculations of statistics such as the correlation coefficient and regression coefficients, as used in the quantification of aerosol-cloud interactions, are relatively well understood; however, these effects are almost never discussed (exceptions to be discussed later) when inference is made from analyses of ACI at varying scales in the literature (Fig. 1).

2.2.1 Scale and ACI calculations

Cloud responses to changes in aerosol are typically represented by power-law functions. Using a linear regression between aerosol and cloud properties $y = a + bx$, where y is the logarithm of the cloud property (dependent variable) and x is the logarithm of the aerosol property (independent variable), ACI is simply an estimator of the regression slope b, which can be defined as

$$\hat{b} = r_{xy}\frac{s_y}{s_x} \text{ or ACI} = r_{\text{aerosol,cloud}}\frac{s_{\text{cloud}}}{s_{\text{aerossol}}} \quad (2)$$

ACPD
11, 26741–26789, 2011

The correlation coefficient is

$$r_{xy} = \frac{\mathrm{COV}(xy)}{s_x s_y} \tag{3}$$

with COV(x,y) the covariance between x and y, and s_x the standard deviation of n samples of variable x with mean $\bar{x}$. The standard deviation, the square root of the variance s^2, is

$$s = \sqrt{\frac{\sum_i (x-\bar{x})^{-2}}{n-1}} \tag{4}$$

Hence, changes in ACI with aggregation will be a function of the relative rate of change in the variance of each of the logarithms of aerosol and cloud properties employed and in the change in covariance between the two. It will be shown that the rate of change in s^2 with aggregation or scale changes is dependent on the characteristics and the distributions of the properties of interest.

Numerous empirical studies addressing the MAUP have shown that increasing the level of aggregation results in a loss of variance, leading to an increase in r_{xy} (Openshaw, 1984; Fotheringham and Wong, 1991; Amrhein, 1995). In fact, the literature shows that almost any value of r can be obtained for a dataset by averaging to different degrees over space and time. Studies addressing aerosol-cloud interactions have presented r or r^2 alone or with ACI as evidence of indirect effects, which may be misleading, depending on the level of aggregation of the data considered. Spread in the data may vary depending on whether factors other than aerosol concentration are driving variability in cloud properties. The correlation is not a measure of the degree of the association between aerosol and cloud properties, only a measure of how completely variations in aerosol affect variations in cloud properties.

Sekiguchi et al. (2003) provide an example from AVHRR data that are successively averaged in space and time, showing that with aggregation, r increases rapidly (see their Fig. 2). They argue that more highly aggregated data provide a better estimate of

ACPD
11, 26741–26789, 2011

the effect due to a higher correlation. While r represents the goodness-of-fit of a linear regression model in this case, it cannot necessarily be used as an indicator of the best scale at which to analyze the relationship between aerosol and cloud. We will provide evidence that while disaggregated data may exhibit a wider spread, the fit to this data more accurately represents aerosol-cloud processes and that r or r^2 should not be used as a criterion in determining the fitness of datasets for quantifying the albedo effect.

If the data are properly constrained by cloud liquid water when performing calculations, the quantification of the albedo effect from disaggregated data by the regression slope, regardless of their spread, will be more accurate because measurements were made at the scale of the process. Confidence in that measure should be evaluated by a statistical significance test (p-value) of the regression, regardless of the correlation coefficient, although the two are generally related. Grandey and Stier (2010), in testing the sensitivity of ACI to aggregation of MODIS data, show that as spatial resolution decreases (becomes coarser), the number of statistically significant regressions across the globe increases substantially. Their exercise illustrates how care must be taken in interpretation of results given the nature of the data used for the analysis.

2.2.2 Measurements and ACI calculations

Measurement approach dictates whether data is disaggregated or aggregated and also the degree of aggregation. In any approach to observation, instrument resolution is dependent on limitations generated by integration time and sensor field-of-view. In the case of aerosol or cloud drop concentration, in situ data are generally disaggregated data, as the basic unit of measure is the particle. Temporal resolution is often maximized for in situ observations, within instrumental constraints, as the interest is typically on the microphysical scale. Ground-based and space-based remote sensing produce aggregated data in the form of bulk properties (an average measure of particles, e.g. cloud optical depth) with ground-based data having the potential for much finer resolution. Point-based remote sensing from the ground at high temporal resolution can

ACPD
11, 26741–26789, 2011

capture changes in the microphysical and optical properties at a scale that resolves the processes of interest and thus may be considered a proxy for disaggregated data. For satellite-based sensors, the basic areal unit of study, the pixel, tends to be arbitrary relative to the process being studied, and is based rather on general optimization of the sensor. For each of these types of observation, the basic units of measure are 'modifiable' through the use of statistical methods for upscaling or aggregation of the data. This is often the case with operational products where retrievals require some amount of averaging or with global coverage products that are much more reasonably distributed and examined at coarser resolutions.

By progressively increasing the level of aggregation of data, the heterogeneity in either the aerosol or cloud microphysical variable internal to the sampling unit is lost. Additionally, the influence of other variables (e.g. L or vertical air velocity w, which drive supersaturation production and drop activation) may be changed by enlarging the area over which these other parameters contribute. If they are not controlled for, e.g. by constraining L, the resulting measures may reflect those of multiple processes, and result in ambiguity.

The most accurate values of ACI will result from calculations employing L-constrained, disaggregated data. However, we wish to implement this knowledge at the global scale for which the required fine resolution of either observations or models is not feasible and for which the operational products from satellite sensors are convenient. Below, we provide some illustrations of the impact of scale on quantifying the albedo effect that address the above dilemma. If we are to exploit data over a wide range of scales, from in situ to global coverage using satellite-based sensors, an understanding of the associated error is required. The following discussion is intended to illuminate the primary causes of that error.

ACPD
11, 26741–26789, 2011

3 Methods

To illustrate the potential effects of aggregation on the statistical properties of data, we use a range of data sources over the northeast Pacific Ocean. Our data sources are associated with the marine stratocumulus cloud regime, and derive from the Dynamics and Chemistry of Marine Stratocumulus Phase II (DYCOMS II) experiment (Stevens et al., 2003), which took place off the coast of southern California in July of 2001, as well as the DOE deployment to the northern coast of California in 2005. We draw from cloud-resolving model output, ground-based in situ and remote sensing, and satellite-based remote sensing products of aerosol and cloud properties from the Moderate Resolution Imaging Spectroradiomenter (MODIS) sensor aboard the Terra satellite. A description of the various data sources and pertinent information is provided here.

3.1 Disaggregated data: Pt. Reyes surface observations

High-resolution surface observations are used as a proxy for disaggregated data as previously indicated. Measurements of aerosol and cloud properties are taken from the Department of Energy deployment of the Atmospheric Radiation Measurement (ARM) Mobile Facility to Pt. Reyes, CA that ran from March to September of 2005. Near-continuous in situ observations of aerosol and cloud properties as well as radiometer observations of L are available along with daytime observations of τ_c at a temporal resolution of 20 s. These data are used to produce daily, high temporal resolution correlation statistics between aerosol and cloud properties.

3.2 Aggregated data: MODIS

MODIS scenes from 20 July 2001, during the DYCOMS II experiment, are used as examples of aggregated data. The scenes are located just off the California coast over the DYCOMS II operating region and extending over a larger area of the northeast Pacific. Level 2 data are used which provides instantaneous cloud properties at 1 km

ACPD
11, 26741–26789, 2011

(Platnick et al., 2003) and aerosol properties at 10 km (Remer et al., 2005) resolution, as well as daily averaged Level 3 global coverage data at 1 degree resolution.

3.3 Cloud-resolving model output

Model output is especially useful for exploring scale effects on quantifying aerosol-cloud interactions since, unlike most observations, co-located variables required for the calculations are present in each grid cell and at each time step. We use model output from the Weather and Research Forecasting (WRF) Model run in cloud-resolving mode (Wang and Feingold, 2009) to illustrate the effects of data aggregation on ACI. The WRF model was implemented using environmental parameters from the DYCOMS II experiment. Simulations were made on 300 m (horizontal) × 30 m (vertical) grids over a 60 × 60 km domain with a time step of two seconds. Snapshots of model output are examined at 15 min intervals. Cloud optical depth τ_c from the native WRF runs are shown in the top row of Fig. 4. The three separate instances (a, b, and c) represent different aerosol concentrations N_a and temporal evolutions (t) as follows: (a) $N_a = 500\,\mathrm{cm}^{-3}$, $t = 3\,\mathrm{h}$, (b) $N_a = 500\,\mathrm{cm}^{-3}$, $t = 6\,\mathrm{h}$, (c) $N_a = 150\,\mathrm{cm}^{-3}$, $t = 9\,\mathrm{h}$. These different instances result in cloud fields in various stages of open and closed cell development with distinct patterns and distributions of cloud properties.

3.4 PDF sampling for ACI estimation

The WRF model runs were all initialized with a constant aerosol concentration N_a across the domain so that there is little spatial and temporal variability in N_a, except in strongly precipitating conditions. However, in order to calculate correlations between cloud and aerosol properties, as well as ACI, a range of N_a must be present. To achieve this, we ignore the N_a used to generate the simulations and instead use a randomly generated normal distribution of N_a with a mean at the initial modeled N_a. Next we build a joint L and updraft velocity w distribution using the WRF output. Using a method of random sampling that accesses all possible combinations of the N_a and joint L; w

Discussion Paper | Discussion Paper | Discussion Paper | Discussion Paper |

ACPD

11, 26741–26789, 2011

The scale problem in quantifying aerosol indirect effects

A. McComiskey and G. Feingold

probability distribution functions (PDF), each set of N_a, L and w are used as input to an adiabatic cloud parcel model (Feingold and Heymsfield, 1992) to produce a proxy data set for τ_c (N_d and r_e). A flowchart representing this method is given in Fig. 4. Since the random generation of N_a distributions and the sampling approach results in slight variations in the value of ACI with each separate realization, averages are taken to achieve a robust estimate of ACI. Each data point in an ACI calculation shown in this study is an average from a set of $n = 30$ realizations of the parcel model run on 30 uniquely generated PDFs of N_a.

This method of sampling data in conjunction with the use of a process-scale model provides a comprehensive data set of well distributed N_a, L, and τ_c from which to calculate and explore the impacts of aggregation and other data constraints on ACI. Note that application of this methodology does not preserve the original τ_c PDF in the WRF simulations because a PDF of N_a has been applied to generate the PDF of τ_c; nevertheless, average τ_c is similar. This does not detract from the results since the illustrative nature of these exercises is key.

We will apply this methodology in Sect. 4 and also explore extended applications of this approach in semi-empirical quantifications and model parameterizations of the cloud-albedo effect, in Sect. 5.

4 Observational biases in ACI

WRF model output is used to illustrate the basic effects of aggregation on statistics of cloud microphysical properties. Progressive aggregation of the WRF-derived τ_c field from the original resolution of 0.3 km to 6 km (Fig. 5) results in changes in several basic statistical parameters. Note the different scale bars and decrease in range (the difference between maximum and minimum values of τ_c) with each level of aggregation in Fig. 5. The scene s^2, and τ_c probability distribution functions PDFs for each of these scenes are provided in Fig. 6. The homogeneity parameter $\gamma = (\mu/s^2)$ (Barker, 1996; Wood and Hartman, 2006), where μ is the mean and s is the standard deviation of τ_c, is included in addition to s^2 in reference to several other studies that use this parameter.

ACPD
11, 26741–26789, 2011

As expected, the scene variance decreases and homogeneity increases as the level of aggregation increases. As a result, the PDF becomes narrower and more peaked with progressive aggregation. A narrowing of the PDFs with aggregation (Fig. 6) occurs in response to the loss of variance, but the degree and level of aggregation at which this occurs is dependent on cloud morphology. For instance, by visual inspection of Fig. 4a, it is evident that the clouds have a characteristic length scale of ~2–3 km. In Fig. 4c, the characteristic length scale is ~20 km. In Fig. 6, a distinct threshold in γ and the PDF for Fig. 4a is reached near the characteristic length scale of 2.4 km, with a more subtle change reached in s^2 at that scale. For Fig. 4c, no such threshold is evident in Fig. 6 up to an aggregation level of 6 km. Constraints on the domain size of the WRF runs do not permit further aggregations. The change in these parameters is nonlinear with scale and different for the three different cloud regimes in accord with the level of organization and characteristic length scales of the cloud features. The specific impacts of varying organization and cloud field morphology on statistical parameters will be discussed further in the following section.

Figure 7 provides the correlation coefficient between N_a and τ_c from the PDF sampling outlined in Fig. 5. The correlation coefficient r shows a dramatic increase with aggregation as expected from previous discussions, with the amount of increase varying with the correlation length scale of cloud features in each of the scenes from Fig. 4a–c. Despite theoretical (Eq. 2) and empirical evidence that aggregation leads to an increase in r_{xy}, which would lead to an increase in the slope parameter, we see the "opposite" in published values specific to ACI calculations as data sources move from in situ airborne and ground-based remote sensing to satellite studies with increasingly coarse resolutions (Fig. 1b). Why is this the case? It will be shown that two factors specific to the quantification of the albedo effect produce the dampening trend of ACI with decreasing resolution as seen in the literature: (1) the separation between retrieved aerosol and cloud properties in horizontal space in passive satellite remote sensing products and (2) the lack of constraint on L when performing ACI calculations.

ACPD
11, 26741–26789, 2011

4.1 Separation in horizontal space between aerosol and cloud properties

Many airborne field campaigns have measured near-coincident in situ aerosol and cloud microphysical properties (e.g. Twomey, 1974; Twohy et al., 2005 and refs therein) or have used stacked aircraft to assess the cloud albedo effect by measuring reflectance in a single column (Brenguier et al., 2003; Roberts et al., 2008). Measurements of aerosol-cloud interactions using ground-based remote sensing in a single column of air have been made using Raman lidar extinction of sub-cloud aerosol (Feingold et al., 2003) or surface aerosol alternatives (e.g. Garrett et al., 2004; Kim et al., 2008; Lihavainen et al., 2008; McComiskey et al., 2009) together with r_e retrieved from cloud radar and microwave radiometer to assess the effect in a column of air. In these approaches, instantaneous, co-located measurements of aerosol and cloud properties in a single column improve confidence that the aerosol population measured is that with the potential to impact the cloud properties measured.

The primary source of aerosol and cloud properties used in studies intended to provide a global perspective are space-based, passive remote sensors. However, co-located retrievals of aerosol and cloud properties from these sensors are not physically possible and an assumption is made that the aerosol is sufficiently homogeneous such that measurements made between clouds are representative of the aerosol feeding into the cloud from below. Even with this assumption, there is potential for aerosol measurements between clouds to be contaminated by humidification, cloud fragments, and enhanced photon scattering (see e.g. discussion in Koren et al., 2009), although these issues are not addressed here. When separated in space or time, the relationship between the measured aerosol concentration and assumed resulting cloud microphysics are likely less representative of actual relationships. The extent to which this separation error degrades results depends on the heterogeneity of the aerosol and cloud property distribution in space.

The Level 2 MODIS scene in Fig. 8 illustrates the separation between aerosol optical depth and cloud optical depth that might be used in an analysis of the albedo effect.

Discussion Paper | Discussion Paper | Discussion Paper | Discussion Paper |
ACPD
11, 26741–26789, 2011
The scale problem in quantifying aerosol indirect effects
A. McComiskey and G. Feingold

There is no information on the variation in aerosol amount in the locations of elevated τ_c such as the ship tracks seen in the upper center portion of the scene. At this scale it is clear that the aerosol properties are not complete with respect to the location of cloud to meet the criteria of a process-scale analysis. While MODIS Level 2 data provide instantaneous properties with global coverage, they are generally not used in global-scale analyses due to the volume of data that would be required. More often, Level 3 daily averaged data produced on a regular, 1-degree grid are used for these analyses.

With passive satellite remote sensing where aerosol and cloud can not be measured simultaneously, such aggregation of aerosol and cloud properties over larger areas (time periods) allows for the population of grid cells (regular time steps) with measured values, where previously there were missing values. Computationally, this provides co-located properties where they may not have existed at finer resolution. However, this computational aggregation may not preserve statistical accuracy in the variables. This phenomenon can be observed in the MODIS Level 3 images in Fig. 9 as compared to the images in Fig. 8 where the insets in Fig. 9 represent the same area of the scenes in Fig. 8. Co-located aerosol and cloud optical depths increase greatly in the Level 3 data but the values also change, becoming more homogeneous.

Levy et al. (2009) showed that different approaches to averaging MODIS data for monthly average aerosol optical depth products produce different empirical results, sometimes by more that 30 %. This is due to different sampling issues caused by the satellite orbital geometry, limitations of the retrieval algorithm in some conditions such as, but not limited to, cloud cover, and the consequent weighting strategies used to account for these issues. One exercise showed that monthly averaged values were dampened systematically by 10 % compared to daily averaged values. Depending on the approach taken to averaging, the results may vary enough to bias quantification of indirect effects appreciably.

The amount of separation between individual, retrievable aerosol and cloud observations in any given analysis using passive remote sensors will depend on cloud fraction and so the bias will, again, be dependent on cloud regime. Commonly, stratiform

ACPD
11, 26741–26789, 2011

clouds have been targeted for airborne and ground-based studies of the cloud-albedo effect not only for their continuous cover and amenability to sampling, but also for their importance in affecting global radiative forcing and climate sensitivity. These clouds provide conditions for more accurate analyses from ground-based and in situ observations but, because of their high relative cloud fraction, stratiform clouds would produce the largest biases in satellite analyses due to separation. Grandey and Stier (2010) found that errors in quantifying the albedo effect from space were most notable in stratocumulus regions due to variability in aerosol and cloud properties that could not be resolved as spatial resolution decreased.

The effect of separation between individual observations of retrieved aerosol and cloud properties is most easily quantified with high temporal resolution ground-based remote sensing data taken from the ARM Mobile Facility, Pt. Reyes deployment. The data in Fig. 10 is representative of the same cloud regime used to initialize the WRF model runs employed in this study, thus the cloud characteristics are very similar. N_d was calculated from τ_c and L (e.g. Bennartz, 2007) originally sampled at 20 s while N_{CCN}, assumed to vary more slowly, was originally sampled at 30 min then resampled to match the sampling frequency of N_d. To investigate the effect of separation, we apply increasing lag times between aerosol and cloud data and calculate their cross-correlation. The correlation between N_d and N_{CCN} at zero lag time is $r = 0.38$. The cross-correlations at increasing lag times show that the correlation is reduced by nearly half (to $r = 0.18$) over a period of 30 min, or over a distance of 10–20 km depending on a range of wind velocities between 5–10 m s^{-1} used to approximate distance from time (McComiskey et al., 2009). The correlation is near zero after a lag time of 60 min.

Anderson et al. (2003) examined the variability of aerosol properties over space/time from ground, air, and space to better implement synergy among observational approaches and modeling of aerosol impacts on global climate. They found that significant variability occurs on horizontal scales of 40–400 km and temporal scales of 2–48 h. Separation (and/or aggregation) across larger areas would dampen the signal in calculations of indirect radiative forcing by aerosols. At scales smaller than this, it

ACPD
11, 26741–26789, 2011

A. McComiskey and G. Feingold

might be safe to assume that the aerosol adjacent to clouds is a good proxy for that between the clouds (neglecting cloud contamination of the aerosol measurement). The range of 40–400 km is large, however, and spans the bulk of resolutions used in studies of ACI (see Fig. 1b).

In a comparison of L retrievals from ground-based microwave radiometers and space-based sensors, Schutgens and Roebeling (2009) found that the errors due to poor collocation of the sensors, including offset and field-of view differences dominated those due to other factors, such as differences in retrieval algorithms. Interestingly, as space-based resolution increased, errors actually increased rather than decreased if sensor offsets were not accounted for, showing a sensitivity to small-scale variability in L. Wood and Hartmann (2006) found the dominant scales of L variability to be between 10–50 km, resolvable by sensors from all types of platforms but smaller than the typical scales of $\geq 1^{\circ}$ for satellite analyses made from global products with useful, continuous global coverage.

Mathematically, separation will tend to decrease the correlation between aerosol and cloud properties, which will decrease the slope parameter, or ACI. When aggregation is used to improve the frequency of co-located aerosol and cloud properties the effect on ACI may be variable and depend on the individual set of distributions, but the likely rapid loss in correlation due to separation would lead to lower ACI values. The variable errors produced by separation of aerosol and cloud measurements in space and time using different measurement approaches poses a problem when evaluating satellite analyses by ground-based or in situ observations. Evaluating results from this range of different measurement approaches within the same context requires a consideration of scale-specific biases for each approach.

4.2 Ignoring the constraint on cloud liquid water path

Cloud optical depth and reflectance are highly correlated with L (Schwartz et al., 2002; Kim et al., 2003). Various factors including meteorology and cloud drop microphysical properties can result in variability in τ_c. By constraining changes in τ_c by L, the

ACPD
11, 26741–26789, 2011

remaining variability will be due primarily to changes in microphysical properties associated with variation in aerosol. Without this constraint, larger-scale meteorological processes that produce variability in L and therefore τ_c will confound detection of aerosol-cloud interactions.

The constraint of L when calculating ACI is often ignored in satellite-based analyses due the difficulty in achieving an independent measure of L coincident with other cloud and aerosol properties. When unconstrained, the regression slope is flattened due to the spread of uncorrelated aerosol and cloud parameters across different L values that exist in varied meteorological conditions. This was shown using ground-based observations from Pt. Reyes (McComiskey et al., 2009). Here, the PDF sampling methodology described in 3.4 is applied to WRF model output to illustrate the impact of ignoring the constraint of L when quantifying ACI and to show the robustness of this result.

Figure 11 represents all of the data points from Fig. 5b at its native (highest) resolution. Each variable is grouped based on $10\,\mathrm{g\,m^{-2}}\,L$ bins and the colored data represent a sample of those bins. ACI is calculated based on the method outlined in Sect. 3.4 and the flow diagram in Fig. 5. Independent calculations of ACI are made using the N_a and τ_c data from each bin and also for the full set of data in the scene, unconstrained by L. The unconstrained ACI value of 0.16 is lower than any of the constrained values of 0.22, 0.26, and 0.32. If an averaged ACI is calculated from each of the independent L bins, weighted by the number of data points in each bin, the value is 0.22.

Plane parallel radiative transfer calculations following McComiskey and Feingold (2008) shown in Fig. 2 indicate that the difference in constrained versus unconstrained ACI would result in a difference in local (100 % cloud cover) radiative forcing of the cloud albedo effect of approximately $3\,\mathrm{Wm^{-2}}$ (given a change in CCN from 100 to $300\,\mathrm{cm^{-3}}$, $L = 125\,\mathrm{g\,m^{-2}}$) or approximately $0.75\,\mathrm{Wm^{-2}}$ for a globe with a 25 % liquid water cloud fraction, discounting 3-D radiative transfer effects. This is a potentially important source of bias in observationally based radiative forcing estimates of the albedo effect.

ACPD
11, 26741–26789, 2011

A. McComiskey and G. Feingold

With progressive aggregation of data, the result above holds until the statistical properties of the cloud and aerosol data become too altered to allow for a valid ACI calculation. Figure 12 shows the constrained and unconstrained ACI values at each level of aggregation for the three scenes in Fig. 4 (top row). A distinct feature is that the difference between constrained and unconstrained ACIvalues increases as the heterogeneity within the cloud field increases (Fig. 4, top row) from the relatively homogeneous case of closed cells in Fig. 4a to the open cell, highly organized case of Fig. 4c. This is clearly an effect of the increasingly disparate values of L within each scene. The small difference between constrained and unconstrained ACI values in Fig. 4a for the highest level of aggregation is consistent with the high homogeneity parameter for this case (Fig. 6).

The amount of bias that cloud field heterogeneity produces in quantifying the albedo effect is based on the analysis scale and heterogeneity of the measured property internal to that unit of observation. In a homogeneous scene, aggregation of properties results in a relatively accurate representation of the finer-scale properties and processes. However, as organization and pattern become more distinct and complex, aggregation will cause loss of information associated with that pattern. On even larger scales, global studies using satellite-based observations lump various cloud types with widely varying patterns, as well as aerosol with varying properties, by aggregating over regularly gridded data (Grandey and Stier, 2010). In such cases, the trend of increasing differences between ACI constrained and unconstrained by L with scene heterogeneity could result in unconstrained ACI values that are biased very low, such as the analyses that fall to the right of the plot in Fig. 1b with resolutions on the order of 5°.

The trend in ACI with increasing aggregation shown in Fig. 12 is generally flat with some distinct exceptions. Most notably, the unconstrained values are less than the constrained values in all but a couple of cases. The exceptions occur only at high level of aggregation. A closer look at the data reveals that, for these particular exceptions, the ranges of variability of aerosol and cloud properties have become too narrow with aggregation to provide a physically meaningful regression slope.

ACPD
11, 26741–26789, 2011

In this example, larger ACI values are typically a function of narrowed distributions that occur with aggregation, similar to the narrowing of the τ_c PDFs in Fig. 6. Similar results were found for the ground-based data from Pt. Reyes in which the days that had low variability in aerosol concentrations did not provide useful ACI values because distributions were too narrow to achieve a meaningful regression slope (McComiskey et al., 2009). Here we see that the same result can occur from artificially narrowing distributions through aggregation. Generally, this affects data sets in which sample numbers are limited and is not encountered in global scale analyses for which the number of samples is adequate. In the case of global analyses, ACI is most often dampened due to the lack of constraint on L and separation between measured aerosol and cloud properties.

Looking into the individual realizations that make up the ACI values in Fig. 12 provides valuable information for understanding the issues associated with calculating ACI with less-than-ideal data sets. Figure 13 contains the individual ACI calculations (based on Sect. 3.4) from the scene in Fig. 4c, top row for the constrained and unconstrained values at the finest (0.3 km) and coarsest (6 km) resolutions. The set of realizations is stable for both the constrained and unconstrained calculations at 0.3 km resolution and fall within the physically meaningful limits of the relationship Eq. (1a) between 0 and 0.33. With substantial aggregation to 6 km, spurious values of ACI appear for both constrained and unconstrained calculations, but more so for the unconstrained calculations. This is due to the fact that aggregation results in fewer data points from which to calculate a regression slope, resulting in an ACI value that is not robust.

In general, this exercise has shown that unconstrained ACI values tend to be lower than properly calculated, constrained values. While the use of unconstrained values is not appropriate for quantifying the albedo effect, the relationships may have a different but equally physically useful meaning. The relationships derived between aerosol and cloud properties without constraint on L are *ipso facto* more representative of the full system of aerosol-cloud interactions feeding back on themselves rather than just the albedo effect. Hence, the range of radiative forcing from observational estimates shown

Discussion Paper | Discussion Paper | Discussion Paper | Discussion Paper |

ACPD

11, 26741–26789, 2011

The scale problem in quantifying aerosol indirect effects

A. McComiskey and G. Feingold

in Fig. 1a (at right) from −0.5 to −3.9 Wm^{-2} may also be more representative of the multitude of aerosol-cloud interactions with feedbacks rather than solely the albedo effect. Appropriately interpreted, this observed quantity could be used effectively with models for diagnosing the broader class of aerosol-cloud interactions.

5 Observationally-based measurement of ACI using regime-dependent PDFs

We have shown that, for processes such as the albedo effect that operate on the microphysical scale, the use of aggregated data results in errors of statistics and sampling, resulting in biases in associated radiative forcing estimates. Additionally, lack of constraints on the analysis, common with the use of aggregated data, results in a low bias. However, disaggregated data does not easily lend itself to global coverage and, for regional-to-global scale studies that can address climate issues, data must be scaled-up in a manner that preserves accuracy. An approach to an observationally-based estimate of the albedo effect that uses data in conjunction with a process model was outlined previously (Sect. 3.4; Fig. 5) and applied to WRF model output in Figs. 11, 12, and 13. It is detailed here in the context of employing observational data rather than the WRF model output. The objective is to devise an observationally-based approach to radiative forcing estimates and to reduce model uncertainty or biases in those estimates. This proposed approach preserves the internal heterogeneity of units of observation though the use of PDFs rather than means.

The methodology is reiterated here with reference to non-precipitating clouds with relatively small influence of drop coalescence processes and related feedbacks such as wet removal of aerosol. To calculate ACI we require PDFs of L (preferably joint with w; see below) and a measure of aerosol concentration. An independent measure of L is desirable, provided it is at a matched scale. The PDFs are randomly sampled and used as input to a cloud parcel model (or parameterization thereof), which yields the associated PDF of τ_c or a proxy (N_d or r_e) that represents the detailed physical processes involved in microphysical-scale aerosol-cloud interactions. The model ensures that processes relevant to drop activation are well represented. The physics included in the model could vary by regime, depending, for example, on cloud type, adiabatic liquid water fraction, and/or aerosol composition. While we have presented this approach with an adiabatic model for simplicity, it could easily be extended to include sub-adiabaticity using either continuous (e.g. Lee and Pruppacher, 1977) or discrete (Krueger et al., 1997) mixing models.

Because of the inherent coupling between L and w, the fidelity of the calculations can be increased if the dependence on the joint distributions of L; w is included, as in Sect. 3. This is especially true under high aerosol loadings where w plays an increasingly important role in influencing the strength of the cloud response to aerosol (Feingold, 2003; McComiskey et al., 2009). Recent efforts combining Doppler radar and microwave radiometer are beginning to produce such PDFs (P. Kollias and E. Luke, personal communication, 2011) but the extent to which these are dependent on cloud regime must be ascertained before they can be applied more generally.

The random sampling of the aerosol and joint L; w distributions described above represents the full range of possible couplings between aerosol, cloud water, and updraft velocity characteristics over a given domain. This provides "co-located" sets of aerosol, cloud optical depth, and cloud liquid water that span the entire range of likely values in a given regime or geographical location. Typical distributions for different cloud regimes in different geographical locations will result in characteristic globally and temporally distributed ACI values.

An example of data sets that could be used with this methodology are PDFs collected over space and time at relatively high spatial resolution, e.g. MODIS Level 2 data at 1–10 km. These provide a representative distribution of the properties that occur at a given location and/or season over the long-term (albeit without vertical velocity) and are, thus, statistically well-constrained. Sampling these full distributions to calculate ACI would provide a result with bounds on the potential strength of the albedo effect and a probable mean value for the effect. As discussed in the previous section, the source of frequency distributions required for this exercise will vary depending on cloud

ACPD
11, 26741–26789, 2011

and aerosol heterogeneity in a particular regime and so must be determined for a set of self-similar geographical locations and seasons.

Both ground- and space-based observations including active and passive remote sensing can contribute to building such distributions and can provide added dimensionality to the data (e.g. precipitating vs. non-precipitating conditions; Lebsock et al., 2008). This might also yield more opportunity to retrieve cloud and/or aerosol properties with optimal estimation techniques (e.g. Feingold et al., 2006). Additionally, high-resolution sensors can be used synergistically with high-coverage sensors to better quantify the biases incurred in the latter. The combination of high- coverage and high-resolution sensors can also be put to use if one considers that coarser resolutions are appropriate for some observables such as radiative flux for climatological applications, while direct measurements of microphysics require finer scales of observations.

The attractiveness of this method is that it is applicable to observational and model-generated properties and can potentially be used in observationally-based radiative forcing estimates as described above, as well as model evaluation and possibly empirical model parameterization. For the latter, distributions of aerosol, cloud, and updraft velocity parameters within a model grid cell can be used to designate an appropriate value of ACI. Computationally, this would provide a less expensive method than activation parameterization schemes but a more accurate approach than global single-value ACI-based estimates. Alternatively, the characteristic globally- and seasonally-determined ACI values from the previously described observationally-based analysis could be used in models in place of a single, global value.

6 Discussion and conclusions

The influence of aerosol on cloud albedo is recognized as a major unknown. It likely results in a cooling of the planet, the magnitude of which is poorly constrained. Our contention is that model estimates of the radiative impacts of the albedo effect that are based on observed aerosol-cloud interaction ACI metrics are biased due to a mismatch

ACPD
11, 26741–26789, 2011

between process and analysis scales. The historic use of a single measure ACI based on data from a range of different observational scales and platforms results in widely varying answers.

Simple numerical aggregation of data to reach a desired geographical scale does not produce the intended, physically meaningful result at that scale. This is readily seen in the literature that addresses the quantification of the microphysical aspect of the albedo effect, as measured here by ACI. The questions raised here extend beyond the albedo effect; the same issues pertain to other metrics of aerosol-cloud interactions such as aerosol-cloud fraction relationships and aerosol impacts on precipitation such as precipitation susceptibility (e.g. Sorooshian et al., 2009). There the problems are even more difficult because, unlike ACI, they are not constrained by simple physical principles Eq. (1).

Several conclusions relevant to biases in calculating ACI across scales can be drawn from the above illustrations.

ACI employed directly in its form presented in Eq. (1) is useful with process-level/small-scale measurements but is not appropriate for quantifying the albedo effect using aggregated/large-scale measurements from passive, space-based remote sensors, especially in the absence of a constraint on L. Ignoring the constraint on L in calculations of ACI for any observational approach produces a dampening of the signal leading to weaker radiative forcing estimates. The magnitude of this bias is dependent on cloud field morphology (cloud regime) and the interaction of the characteristic scale of cloud features and aerosol distributions with the observational or analysis scale. The bias increases with increasing heterogeneity in the cloud scene (i.e. increasing variability in L). Separation between aerosol and cloud properties in space and/or time result in reduced correlation between the parameters and dampened ACI values. Because of these two issues, observed regional-to-global-scale correlations between aerosol and cloud without appropriate constraints on cloud liquid water do not accurately represent the microphysical-scale interactions between aerosol and cloud albedo. This results in biases in radiative forcing estimates of the cloud-albedo effect in GCMs.

ACPD
11, 26741–26789, 2011

The examination of Grandey and Stier (2010) into the impacts of scale on quantifying the albedo effect concluded that successive aggregation of satellite data from resolutions of $1^\circ \times 1^\circ$ to $60^\circ \times 60^\circ$ resulted in an associated radiative forcing that "increased" with coarser resolution. This is in contrast to the ACI results we show in Fig. 1b from studies throughout the literature that span a range of scales. They used a derivation of $N_\mathrm{d} = f(\tau_c$ and $r_\mathrm{e})$ from MODIS that should in principle be independent of L and thus their results were not affected by lack of constraint on L, but predominately by simple aggregation effects as discussed here in Sect. 2. Here, we have focused on the biases that are incurred in calculation of ACI using aggregated data, which includes all satellite-based observations, as opposed to disaggregated data, which better represents the microphysical processes of interest. We find that, in this case, simple aggregation biases are dominated by the effect of separation of aerosol and cloud properties in space and time and the lack of constraint on L, resulting in associated radiative forcings that are "lower" with decreasing resolution. From these two studies it becomes clear that consideration of the scale and approach to quantifying aerosol-cloud interactions is essential, with no simple recipe for doing so.

Alternative approaches to quantifying the albedo effect exist and should be capitalized upon. Alternatives may include the combination of multiple available passive and active space-based sensors with airborne and ground-based measurements, process-scale modeling, and extrapolation of results using disaggregated data to larger-scales. As the errors in these quantifications are related to cloud field morphology, considering these approaches on a regime-dependent basis may help to minimize that error. The use of regime-dependent PDFs of aerosol and cloud properties may also lead to progress in observationally-based estimates of the albedo effect as well as datasets that could be used for model evaluation and parameterization. We have presented a methodology for such an observationally-based assessment of the albedo effect based on sampling of the full range of the PDF of aerosol and the PDF of liquid water path (preferably joint with updraft velocity).

ACPD
11, 26741–26789, 2011

A. McComiskey and G. Feingold

The question of what is the appropriate scale at which to observe and characterize processes related to aerosol-cloud interactions has been posed many times. It is our assertion that to quantify the albedo effect accurately, disaggregated data (in situ measurements) should be used, or data aggregated only up to the scale that heterogeneity in aerosol and cloud properties is preserved within reasonable error bounds (ground-based remote sensing). Accurate measures from aggregated data are possible to the extent that they are constrained by this spatial or temporal heterogeneity. If these critical scales are not taken into consideration, a heterogeneity- (and therefore geographical- or regime-) dependent bias in ACI will result.

Informed studies using aggregated data require an understanding of the characteristic length scales over which cloud and aerosol properties vary. Typical scales of variability for aerosols have been discussed (Anderson et al., 2003), although a much finer resolution of this variability would benefit observational and modeling efforts (P. Stier, personal communication, 2011). Many studies have addressed the properties of cloud spatial variability in reference to dynamics and radiation (e.g. Barker, 2000), but for indirect effects there is the added complexity of assessing the change in covariance properties with the scale of the aerosol and cloud observations. Quantifying length scales of heterogeneity in different cloud regimes to reduce aggregational error in analyses of aerosol-cloud interactions is a non-trivial problem that will require a focused research effort.

With respect to future analyses of this integrated set of indirect effects, it seems intuitive that studying the system of indirect effects as they interact and perhaps moderate (Stevens and Feingold, 2009) one another would include some form of multivariate regression analysis. While the effect of aggregation on univariate and bivariate statistics is somewhat intuitive and relatively well understood, the effects on multivariate statistics is highly complex and no trends or potential solutions have been proffered, to the authors' knowledge, although it is a subject of great interest in other fields of study. Ongoing work is focused on regime dependent differences in cloud organizational structure and morphology relative to aerosol distributions to determine the most

ACPD
11, 26741–26789, 2011

appropriate approaches to characterizing the full range of indirect effects in the system.

Acknowledgements. This research was supported by the Office of Science (BER), US Department of Energy, Interagency Agreement No. DE-SC0002037. We thank Hailong Wang for providing the cloud resolving model fields in Fig. 5.

References

Ackerman, A., Kirkpatrick, M. P., Stevens, D. E., and Toon, O. B.: The impact of humidity above stratiform clouds on indirect aerosol climate forcing, Nature, 432, 1014, doi:10.1038/nature03174, 2004.

Albrecht, B.: Aerosols, cloud microphysics, and fractional cloudiness, Science, 245, 1227–1230, 1989.

Amrhein, C. G.: Searching for the elusive aggregation effect: evidence from statistical simulations, Environ. Plann. A, 27, 105–119, 1995.

Anderson, T. L., Charlson, R. J., Winker, D. M., Ogren, J. A., and Holmen, K.: Mesoscale variations of tropospheric aerosols, J. Atmos. Sci., 60, 119–136, 2003.

Barker, H.: A Parameterization for Computing Grid-Averaged Solar Fluxes for Inhomogeneous Marine Boundary Layer Clouds, Part I: Methodology and Homogeneous Biases, J. Atmos, Sci., 53, 2289–2303, 1996.

Barker, H.: Indirect Aerosol Forcing by Homogeneous and Inhomogeneous Clouds, J. Climat., 13, 4042–4049, 2000.

Bennartz, R.: Global assessment of marine boundary layer cloud droplet number concentration from satellite, J. Geophys. Res., 112, D02201, doi:10.1029/2006JD007547, 2007.

Bony, S. and Dufrense, J.-L.: Marine boundary layer clouds at the heart of tropical feedback uncertainties in climate models, Geophys. Res. Lett., 32, L20806, doi:10.1029/2005GL023851, 2005.

Brenguier, J. -L., Pawlowska, H., and Schuller, L.: Cloud microphysical and radiative properties for parameterization and satellite monitoring of the indirect effect of aerosol on climate, J. Geophys. Res., 108, 8632, doi:10.1029/2002JD002682, 2003a.

Brenguier, J.-L., Chuang, P. Y., Fouquart, Y., Johnson, D. W., Parol, F., Pawlowska, H., Pelon, J., Schüller, L., Schröder, F., and Snider, J.: An overview of the ACE-2 CLOUDYCOLUMN closure experiment, edited by: Tellus B., 52, 815–827, doi:10.1034/j.1600-0889.2000.00047.x., 2003b.

Bréon, F.-M., Tanre, D., and Generoso, S.: Aerosol Effect on Cloud Droplet Size Monitored from Satellite, Science, 295, 834–838, doi:10.1126/science.1066434, 2000.

Bulgin, C. E., Palmer, P. I., Thomas, G. E., Arnold, C. P. G., Campmany, E., Carboni, E., Grainger, R. G., Poulsen, C., Siddans, R., and Lawrence, B. N.: Regional and seasonal variations of the Twomey indirect effect as observed by the ATSR-2 satellite instrument, Geophys. Res. Lett., 35, L02811, doi:10.1029/2007GL031394, 2008.

Feingold, G.: Modeling of the first indirect effect: Analysis of measurement requirements, Geophys. Res. Lett., 30, 1997, doi:10.1029/2003GL017967, 2003.

Feingold, G. and Heymsfeld, A.: Parameterizations of the condensational growth of droplets for use in GCMs, J. Atmos. Sci., 49, 2325–2342, 1992.

Feingold, G., Remer, L. A., Ramaprasad, J., and Kaufman, Y. J.: Analysis of smoke impact on clouds in Brazilian biomass burning regions: An extension of Twomey's approach, J. Geophys. Res., 106, 22907–22922, 2001.

Feingold, G., Eberhard, W. L., Veron, D. E., and Previdi, M.: First measurements of the Twomey indirect effect using ground-based remote sensors, Geophys. Res. Lett., 30, 1287, doi:10.1029/2002GL016633, 2003.

Feingold, G., Furrer, R., Pilewskie, P., Remer, L. A., Min, Q., and Jonsson, H.: Aerosol Indirect Effect Studies at Southern Great Plains during the May 2003 Intensive Operations Period, J. Geophys. Res., 111, D05S14, doi:10.1029/2004JD005648, 2006.

Forster, P., Artaxo, P., Berntsen, T., Betts, R., Fahey, D. W., Haywood, J., Lean, J., Lowe, D. C., Myhre, G., Nganga, J., Prinn, R., Raga, G., Schulz, M., and van Dorland, R.: Changes in atmospheric constituents and in radiative forcing, in Climate Change 2007: The Physical Science Basis-Contribution of Working Group I to the Fourth Assessment Report of the Intergovernmental Panel on Climate Change, edited by: Solomon, S., Qin, D., Manning, M., Chen, Z., Marquis, M., Averyt, K. B., Tignor, M., and Miller, H. L., 289–348, Cambridge Univ. Press, Cambridge, UK, New York, USA, 2007.

Fotheringham, A. S. and Wong D. W.: The modifiable areal unit problem in multivariate statistical analysis, Environ. Plann. A, 23, 1025–1044, 1991.

Garrett, T. J., Zhao, C., Dong, X., Mace, G. G., and Hobbs, P. V.: Effects of varying aerosol regimes on low-level Arctic stratus, Geophys. Res. Lett., 31, L17105, doi:10.1029/2004GL019928, 2004.

ACPD

11, 26741–26789, 2011

The scale problem in quantifying aerosol indirect effects

A. McComiskey and G. Feingold

Grandey, B. S. and Stier, P.: A critical look at spatial scale choices in satellite-based aerosol indirect effect studies, Atmos. Chem. Phys., 10, 11459–11470, doi:10.5194/acp-10-11459-2010, 2010.
Gultepe, I., Isaac, G. A., Leaitch, W. R., and Banic, C. M.: Parameterizations of marine stratus microphysics based on in-situ observations: Implications for GCMs, J. Climat., 9, 345–357, 1996.
Jelinski, D. E. and Wu, J.: The modifiable areal unit problem and implications for landscape ecology, Landscape Ecol., 11, 129–140, 1996.
Kaufman, Y. J., Koren, I., Remer, L. A., Rosenfeld, D., and Rudich, Y.: The effect of smoke, dust, and pollution aerosol on shallow cloud development over the Atlantic Ocean, P. Natl. Acad. Sci., 102, 11207–11212, doi:10.1073/pnas.0505191102, 2005.
Kim, B.-G., Schwartz, S. E., Miller, M. A., and Min, Q.: Effective radius of cloud droplets by ground-based remote sensing: Relationship to aerosol, J. Geophys. Res., 108, 4740, doi:10.1029/2003JD003721, 2003.
Kim, B.-G., Miller, M. A., Schwartz, S. E., Liu, Y., and Min, Q.: The role of adiabaticity in the aerosol first indirect effect, J. Geophys. Res., 113, D05210, doi:10.1073/pnas.0505191102, 2008.
Koren, I., Feingold, G., Jiang, H., and Altaratz, O.: Aerosol effects on the inter-cloud region of a small cumulus cloud field, Geophys. Res. Lett., 36, L14805, doi:10.1029/2009gl037424, 2009.
Krueger, S. K., Su, C.-W., and McMurtry, P. A.: Modeling Entrainment and Finescale Mixing in Cumulus Clouds, J. Atmos. Sci., 54, 2697–2712, 1997.
Lebsock M. D., Stephens, G. L., and Kummerow, C.: Multisensor satellite observations of aerosol effects on warm clouds, J. Geophys. Res., 113, D15205, doi:10.1029/2008JD009876, 2008.
Koren,-I., Feingold, G., Jiang, H., and Altaratz, O.: Aerosol effects on the inter? Cloud region of a small cumulus cloud field, Geophys. Res. Lett., 36, L14805, doi:10.1029/2009GL037424, 2009.
Lee, I.-Y. and Pruppacher H. R.: A comparative study on the growth of cloud drops by condensation using an air parcel model with and without entrainment, Pure and Appl. Geophys., 115, 523–545, doi:10.1007/BF00876119, 1977.
Levy, R. C., Leptoukh, G. G., Kahn, R., Zubko, V., Gopalan, A., and Remer, L. A.: A Critical Look at Deriving Monthly Aerosol Optical Depth From Satellite Data, IEEE T. Geosci. Remote

ACPD
11, 26741–26789, 2011

The scale problem in quantifying aerosol indirect effects

A. McComiskey and G. Feingold

Sens., 47, 2942–2956, doi:10.1109/TGRS.2009.2013842, 2009.
Lihavainen, H., Kerminen, V.-M., Komppula, M., Hyvärinen, A.-P., Laakia, J., Saarikoski, S., Makkonen, U., Kivekäs, N., Hillamo, R., Kulmala, M., and Viisanen, Y.: Measurements of the relation between aerosol properties and microphysics and chemistry of low level liquid water clouds in Northern Finland, Atmos. Chem. Phys., 8, 6925–6938, doi:10.5194/acp-8-6925-2008, 2008.
Lohmann, U., Rotstayn, L., Storelvmo, T., Jones, A., Menon, S., Quaas, J., Ekman, A. M. L., Koch, D., and Ruedy, R.: Total aerosol effect: radiative forcing or radiative flux perturbation?, Atmos. Chem. Phys., 10, 3235–3246, doi:10.5194/acp-10-3235-2010, 2010.
Lu, M.-L., Conant, W. C., Jonsson, H. H., Varutbangkul, V., Flagan, R. C., and Seinfeld, J. H.: The Marine Stratus/Stratocumulus Experiment (MASE): Aerosol-cloud relationships in marine stratocumulus, J. Geophys. Res., 112, D10209, doi:10.1029/2006JD007985, 2007.
Lu, M.-L., Feingold, G., Jonsson, H. H., Chuang, P. Y., Gates, H., Flagan, R. C., and Seinfeld, J. H.: Aerosol-cloud relationships in continental shallow cumulus, J. Geophys. Res., 113, D15201, doi:10.1029/2007JD009354, 2008.
Martin, G. M., Johnson, D. W., and Spice, A.: The measurement and parameterization of effective radius of droplets in warm stratocumulus clouds, J. Atmos. Sci., 51, 1823–1842, 1994.
Matsui, T., Masunaga, H., Kreidenweis, S. M., Pielke, R. A., Tao, W.-K., Chin, M., and Kaufman, Y. J.: Satellite-based assessment of marine low cloud variability associated with aerosol, atmospheric stability and the diurnal cycle, J. Geophys. Res., 111, D17204, doi:10.1029/2005JD006097, 2006
McComiskey, A. and Feingold, G.: Quantifying error in the radiative forcing of the first aerosol indirect effect, Geophys. Res. Lett., 35, L02810, doi:10.1029/2007GL032667, 2008.
McComiskey, A., Feingold, G., Frisch, A. S., Turner, D. D., Miller, M. A., Chiu, J. C., Min, Q., and Ogren, J. A.: An assessment of aerosol-cloud interactions in marine stratus clouds based on surface remote sensing, J. Geophys. Res., 114, D09203, doi:10.1029/2008JD011006, 2009.
McFarquhar, G. M. and Heymsfield, A. J.: Parameterizations of INDOEX microphysical measurements and calculations of cloud susceptibility: Applications for climate studies, J. Geophys. Res., 106, 675–698, 2001.
Medeiros, B., Stevens, B., Held, I. M., Zhao, M., Williamson, D. L., Olson, J. G., and Bretherton, C. S.: Aquaplanets, Climate Sensitivity and Low Clouds, J. Climat., 21, 4974–4991, 2008.

ACPD
11, 26741–26789, 2011

Murphy, D., Solomon, S., Portmann, R., Rosenlof, K., Forster, P., and Wong, T.: An observationally based energy balance for the Earth since 1950, J. Geophys. Res., 114, D1717, doi:10.1029/2009jd012105, 2009.

Nakajima, T., Higurashi, A., Kawamoto, K., and Penner, J. E.: A possible correlation between satellite-derived cloud and aerosol micro-physical parameters, Geophys. Res. Lett., 28, 1171–1174, 2001.

O'Dowd, C. D., Lowe, J. A., Smith, M. H., Kaye, A. D.: The relative importance of sea-salt and nss-sulphate aerosol to the marine CCN population: An improved multi-component aerosol-droplet parameterization, Q. J. Roy. Meteor. Soc., 125, 1295–1313, 1999.

Openshaw, S.: The Modifiable Areal Unit Problem: Concepts and Techniques in Modern Geography, No. 38, 1984.

Platnick, S., King, M. D., Ackerman, S. A., Menzel, W. P., Baum, B. A., Riédi, J. C., and Frey, R. A.: The MODIS Cloud Products: Algorithms and Examples From Terra, IEEE T. Geosci. Remote Sens., 41, 459–473, 2003.

Quaas, J., Boucher, O., and Breon, F.-M.: Aerosol indirect effects in POLDER satellite data and the Laboratoire de Meteorologie Dynamique-Zoom (LMDZ) general circulation model, J. Geophys. Res., 109, D08205, doi:10.1029/2003JD004317, 2004.

Quaas, J., Boucher, O., and Lohmann, U.: Constraining the total aerosol indirect effect in the LMDZ and ECHAM4 GCMs using MODIS satellite data, Atmos. Chem. Phys., 6, 947–955, doi:10.5194/acp-6-947-2006, 2006.

Quaas, J., Boucher, O., Bellouin, N., and Kinne, S.: Satellite-based estimate of the direct and indirect aerosol climate forcing, J. Geophys. Res., 113, D05204, doi:10.1029/2007JD008962, 2008.

Quaas, J., Ming, Y., Menon, S., Takemura, T., Wang, M., Penner, J. E., Gettelman, A., Lohmann, U., Bellouin, N., Boucher, O., Sayer, A. M., Thomas, G. E., McComiskey, A., Feingold, G., Hoose, C., Kristjánsson, J. E., Liu, X., Balkanski, Y., Donner, L. J., Ginoux, P. A., Stier, P., Grandey, B., Feichter, J., Sednev, I., Bauer, S. E., Koch, D., Grainger, R. G., Kirkevåg, A., Iversen, T., Seland, Ø., Easter, R., Ghan, S. J., Rasch, P. J., Morrison, H., Lamarque, J.-F., Iacono, M. J., Kinne, S., and Schulz, M.: Aerosol indirect effectsgeneral circulation model intercomparison and evaluation with satellite data, Atmos. Chem. Phys., 9, 8697–8717, doi:10.5194/acp-9-8697-2009, 2009.

Raga, G. B. and Jonas, P. R.: On the link between cloud-top radiative properties and sub-cloud aerosol concentrations, Q. J. Roy. Meteor. Soc., 119, 1419–1425, 1993.

Ramanathan, V., Crutzen,P. J., Kiehl, J. T., Rosenfeld, D.: Aerosols, climate, and the hydrological cycle, Science, 294, 2119–2124, 2001.
Remer, L. A., Kaufman, Y. J., Tanre, D., Matoo, S., Chu, D. A., Martins, J. V., Li, R.-R., Ichoku, C., Levy, R. C., Kleidman, R. G., Eck, T. F., Vermote, E., and Holben, B. N.: The MODIS Aerosol Algorithm, Products and Validation, J. Atmos. Sci., 62, 947–973, 2005.
Roberts, G. C., Ramana, M. V., Corrigan, C., Kim, D., and Ramanathan, V.: Simultaneous observations of aerosol-cloud-albedo interactions with three stacked unmanned aerial vehicles, P. Natl. Acad. Sci., 105, 7370–7375, doi:10.1073/pnas.0710308105, 2008.
Robinson, W. S.: Ecological Correlations and the Behavior of Individuals, Am. Sociol. Rev, 15, 351–357, 1950.
Rossow, W.:Studying Earth's Climate from Satellite Observations, Abstract A53G-01 presented at 2010 Fall Meeting, AGU, San Francisco, Calif., 13–17 December 2010.
Schutgens, N. A. J. and Roebling, R. A.: Validating the Validation: The Influence of Liquid Water Distribution in Clouds on the Intercomparison of Satellite and Surface Observations, J. Atmos. Ocean. Tech., 26, 1457–1474, doi:10.1175/2009JTECHA1226.1, 2009.
Schwartz, S. E., Harshvardhan, C., and Benkovitz, M.: Influence of anthropogenic aerosol on cloud optical depth and albedo shown by satellite measurements and chemical transport modeling, P. Natl. Acad. Sci, 99, 1784–1789, 2002.
Sekiguchi, M., Nakajima, T., Suzuki, K., Kawamoto, K., Higurashi, A., Rosenfeld, D., Sano, I., and Mukai, S.: A study of the direct and indirect effects of aerosols using global satellite data sets of aerosol and cloud parameters, J. Geophys. Res., 108, 4699, doi:10.1029/2002JD003359, 2003.
Sorooshian, A., Feingold, G., Lebsock, M. D., Jiang, H. L., and Stephens G. L.: On the precipitation susceptibility of clouds to aerosol perturbations, Geophys, Res. Lett., 36, L13803, doi:10.1029/2009GL038993, 2009.
Stevens, B. and Feingold, G.: Untangling aerosol effects on clouds and precipitation in a buffered system, Nature, 461, 607–613 doi:10.1038/nature08281, 2009.
Stevens, B., Lenschow, D. H., Vali, G., Gerber, H., Bandy, A., Blomquist, B., Brenguier, J. -L., Bretherton, C. S., Burnet, F., Campos, T., Chai, S., Faloona, I., Friesen, D., Haimov, S., Laursen, K., Lilly, D. K., Loehrer, S. M., Szymon, P., Malinowski, Morley, B., Petters, M. D., Rogers, D. C., Russell, L., Savic-Jovcic, V., Snider, J. R., Straub, D., Szumowski, M. J., Takagi, H., Thornton, D. C., Tschudi, M., Twohy, C., Wetzel, M., van Zanten, M. C.: Dynamics and Chemistry of Marine Stratocumulus-DYCOMS II, B. Am. Meteorol. Soc., 84, 579–593,

doi:10.1175/BAMS-84-5-579, 2003.
Twomey, S.: Pollution and the planetary albedo, Atmos. Environ., 8, 1251–1256, 1974.
Twohy, C. H., Petters, M. D., Snider, J. R., Stevens, B., Tahnk, W., Wetzel, M., Russell, L., and Burnet, F.: Evaluation of the aerosol indirect effect in marine stratocumulus clouds: Droplet number, size, liquid water path and radiative impact, J. Geophys. Res., 110, D08203, doi:10.1029/2004JD005116, 2005.
Wang, H. and Feingold, G.: Modeling Mesoscale Cellular Structures and Drizzle in Marine Stratocumulus. Part I: Impact of Drizzle on the Formation and Evolution of Open Cells, J. Atmos. Sci., 66, 3237–3256, doi:10.1175/2009JAS3022.1, 2009
Wood, R. and Hartmann, D. L.: Spatial Variability of Liquid Water Path in Marine Low Cloud: The Importance of Mesoscale Cellular Convection, J. Climat., 19, 1748–1764, 2006.
Xue, H., Feingold, G., and Stevens, B.: Aerosol effects on clouds, precipitation, and the organization of shallow cumulus convection, J. Atmos. Sci., 65, 392–406, doi:10.1175/2007JAS2428.1, 2008.

ACPD
11, 26741–26789, 2011

The scale problem in quantifying aerosol indirect effects

A. McComiskey and G. Feingold

Table 1. References used in Fig. 1b. All studies address low or liquid clouds.

		method/instrument	parameters used	ACIτ	resolution	temporal averaging	L*
Ground							
	Feingold et al. (2003)	RS		0.10	20 s		yes
	Garrett et al. (2004)	RS+in situ		0.15	30 min		yes
	Kim et al. (2008)	RS+in situ		0.15	5 min		yes
	Lihavainen et al. (2008)	in situ		0.24	1 h		yes
	McComiskey et al. (2009)	RS+in situ		0.16	20 s		yes
Airborne							
	Twohy et al. (2005)	in situ		0.27	10–60 min		
	Raga and Jonas (1993)	in situ		0.09	NA		no
	Martin et al. (1994)	in situ		0.25	30 km		
	Gultepe et al. (1996)	in situ		0.22	~ 12km		yes
	O'Dowd et al. (1999)	in situ		0.20			
	McFarquhar and Heymsfield (2001)	in situ		0.11			
	Ramanathan (2001)	in situ		0.21–0.33			
	Lu et al. (2007)	in situ		0.19	30 km		
	Lu et al. 2008	in situ		0.14	leg means		
Satellite							
	Nakajima et al. (2001)	AVHRR	N_d ; N_a	0.17	0.5°	4 months	
	Bulgin et al. (2008)	ASTER-2	r_e ; τ_a	0.10–0.16 (0.13)	1°	seasona l/3 months	no
	Kaufman et al. (2005)	MODIS	r_e;AI	0.046–0.174 (0.0975)	1°	simultaneous/daily	no
	Sekiguchi et al. (2003)	AVHRR	r_e ; N_a	0.1	2.5°	daily	no
	Lebsock et al. (2008)	MODIS	r_e ;AI	0.07	1 km to 1°	simultaneous	no
	Sekiguchi et al. (2003)	POLDER	r_e ; N_a	0.07 (ocean)	2.5°	monthly	no
	Quaas et al. (2006)	MODIS	N_d ; τ_a	0.04	3.75° × 5°	daily	
	Quaas et al. (2004)	POLDER	r_e ; AI	0.04 (ocean)/0.012 (land)	3.75° × 5°	simultaneous	no

* L-constraint used in calculation of ACI

ACPD
11, 26741–26789, 2011

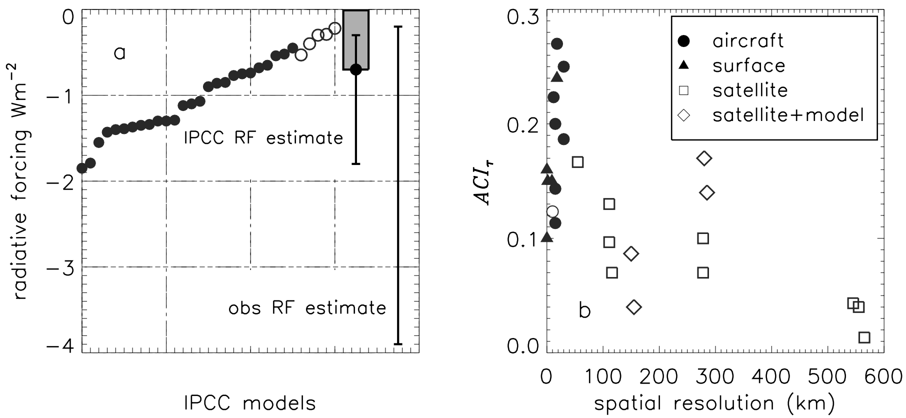

Fig. 1. **(a)** Radiative forcing estimates by each IPCC model and the overall IPCC radiative forcing estimate in comparison to an observational estimate for the cloud albedo effect resulting from the values in **(b)**. **(b)** Values from the literature quantifying the albedo effect using some variant of Eq. (1), expressed here as ACI_τ, and plotted as a function of scale (resolution) of the study. Closed symbols are those that calculate the original variant of ACI with constraint on cloud water and open symbols are those that ignore the constraint on cloud water.

ACPD

11, 26741–26789, 2011

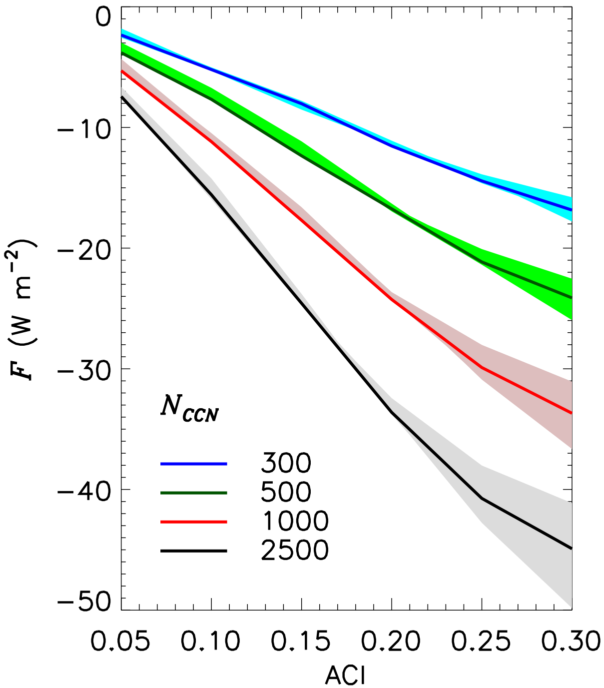

Fig. 2. The amount of forcing as ACI_τ varies across the observed range in Fig. 1b. Values for forcing are given for the difference of four different N_{CCN} concentrations from $N_{CCN} = 100\,cm^{-3}$ and the shaded envelopes represent the range of forcing for each of these concentrations for a range of L from 50–200 $g\,m^{-2}$.

ACPD
11, 26741–26789, 2011

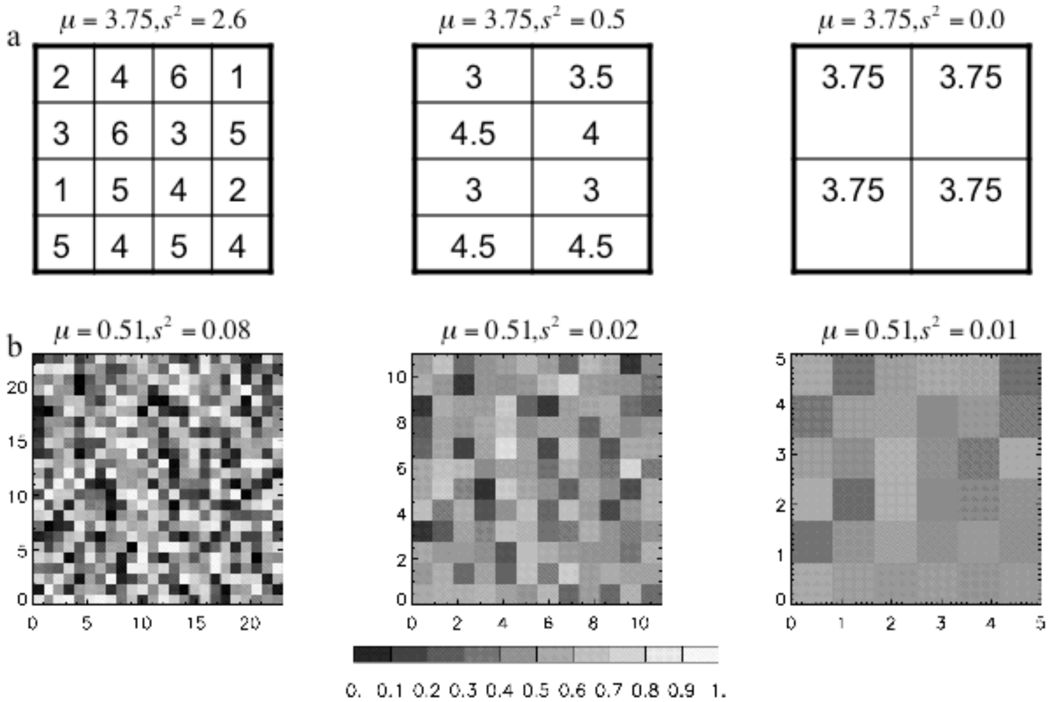

Fig. 3. Change in variance s^2 with aggregation of two simple datasets **(a)** from Jelinski and Wu (1996) and **(b)** randomly generated numbers. Note the constant value for the mean μ in each case as the variance decreases with aggregation.

ACPD
11, 26741–26789, 2011

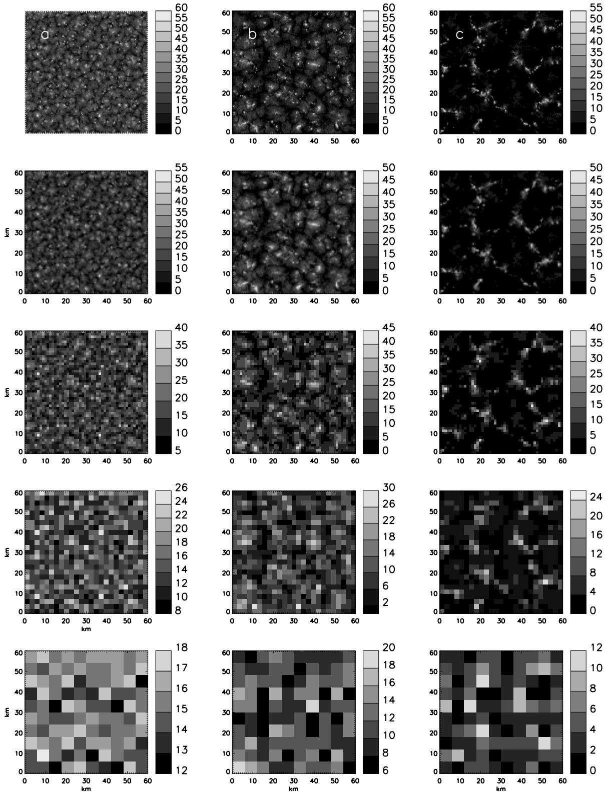

Fig. 4. Modeled τ_c for three aerosol conditions and stages of temporal evolution: **(a)** $N_a = 500\,cm^{-3}$, $t = 3\,h$, **(b)** $N_a = 500\,cm^{-3}$, $t = 6\,h$, **(c)** $N_a = 150\,cm^{-3}$, $t = 9\,h$. The five levels of aggregation represent resolutions of 0.3, 0.6, 1.2, 2.4, and 6 km.

ACPD
11, 26741–26789, 2011

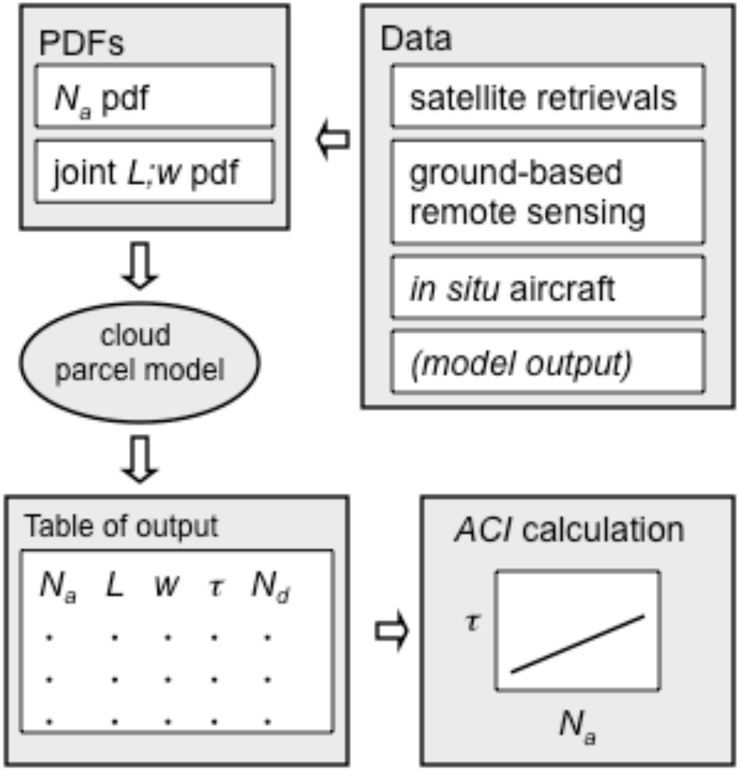

Fig. 5. Flow chart of the random sampling method for a semi-empirical approach to ACI calculations. PDFs for input to a process-scale model can be built from a variety of sources including model output and measurements made at a range of scales.

ACPD
11, 26741–26789, 2011

The scale problem in quantifying aerosol indirect effects

A. McComiskey and G. Feingold

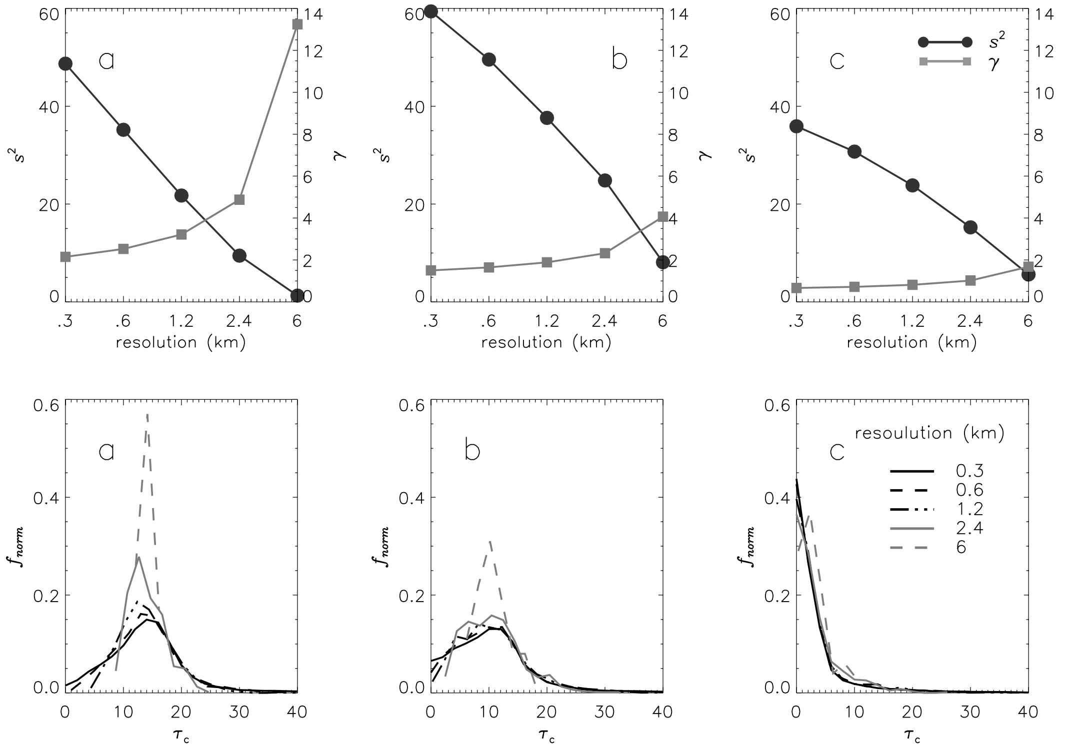

Fig. 6. Statistical parameters variance s^2, homogeneity parameter γ, and PDFs of τ_c for the native resolution and aggregated scenes **(a)**, **(b)**, and **(c)** in Fig. 4.

ACPD
11, 26741–26789, 2011

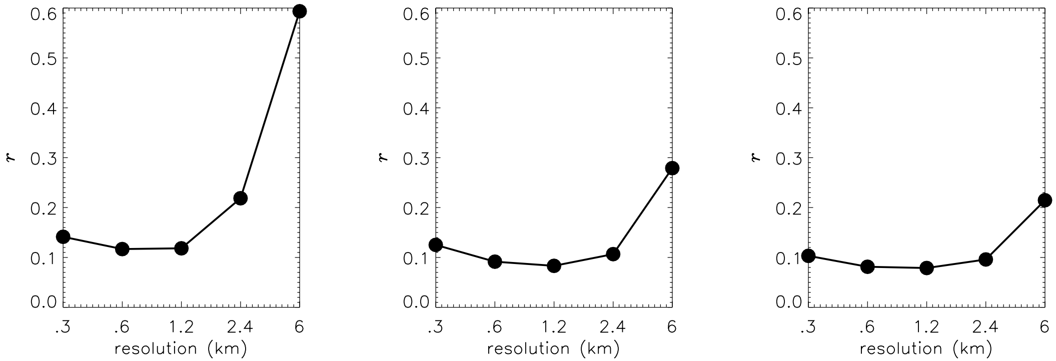

Fig. 7. Statistical parameter r for τ_c vs. N_d for the native resolution and aggregated scenes from **(a)**, **(b)**, and **(c)** in Fig. 4.

ACPD
11, 26741–26789, 2011

The scale problem in quantifying aerosol indirect effects

A. McComiskey and G. Feingold

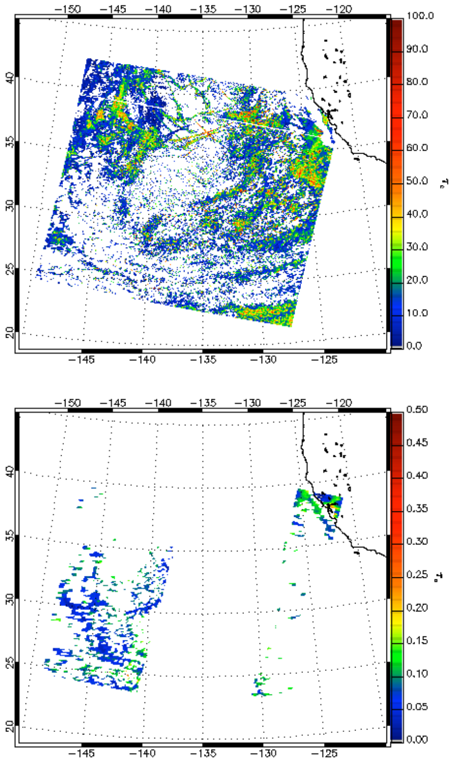

Fig. 8. MODIS Level 2 data over the northeast Pacific Ocean on 20 July 2001: cloud optical depth (top) at 1 km resolution and aerosol optical depth (bottom) at 10 km resolution.

ACPD
11, 26741–26789, 2011

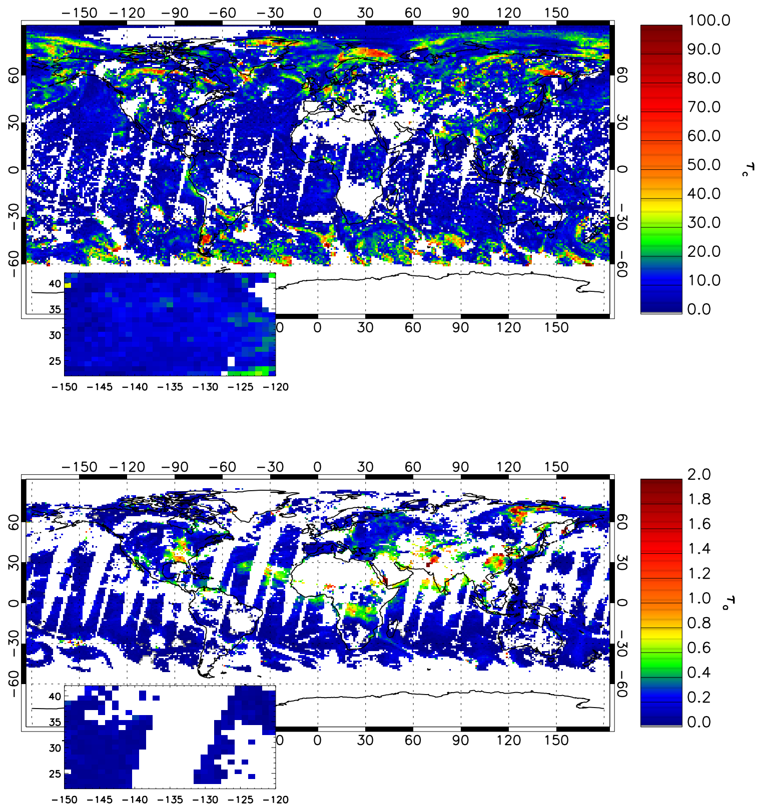

Fig. 9. MODIS Level 3 global data on 20 July 2001: cloud optical depth (top) and aerosol optical depth (bottom), both at 1-degree resolution. The insets represent the same area as the scenes in Fig. 8 over the northeast Pacific Ocean.

ACPD
11, 26741–26789, 2011

The scale problem in quantifying aerosol indirect effects

A. McComiskey and G. Feingold

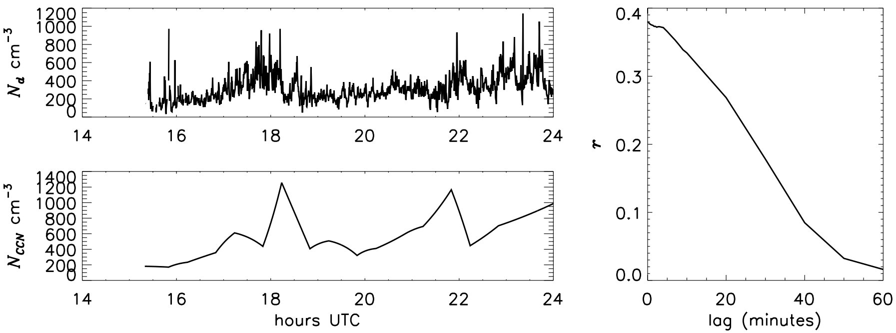

Fig. 10. Lagged cross-correlation of N_d and N_CCN from the DOE Pt. Reyes ARM Mobile Facility deployment in 2005.

ACPD
11, 26741–26789, 2011

The scale problem in quantifying aerosol indirect effects

A. McComiskey and G. Feingold

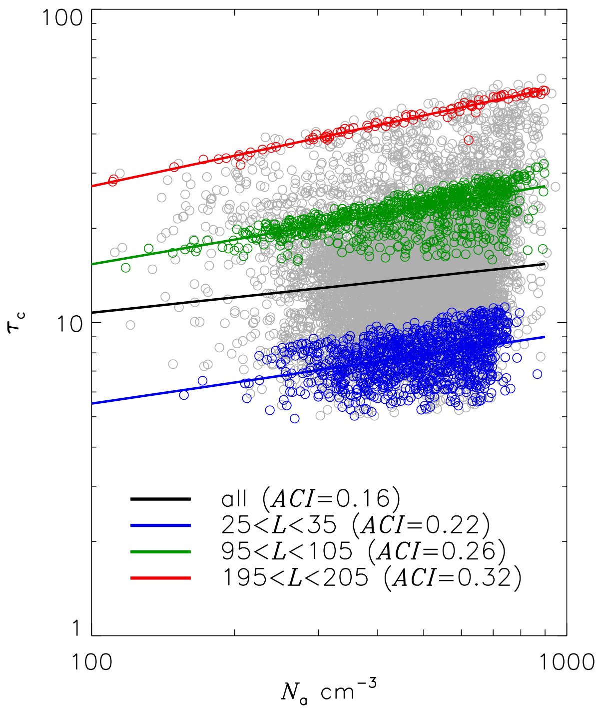

Fig. 11. Pairs of N_a and τ_c produced by a parcel model following the PDF sampling method in Fig. 5 using aerosol and cloud property inputs derived from the high resolution case of WRF scene **(b)** in Fig. 4. Grey symbols represent all data points from the modeled scene and colored symbols represent selected $10\,\mathrm{g\,m^{-2}}$ L bins. The black line represents the unconstrained slope or ACI resulting from all data points and the colored lines represent the slopes for that L bin, or selected constrained ACI values.

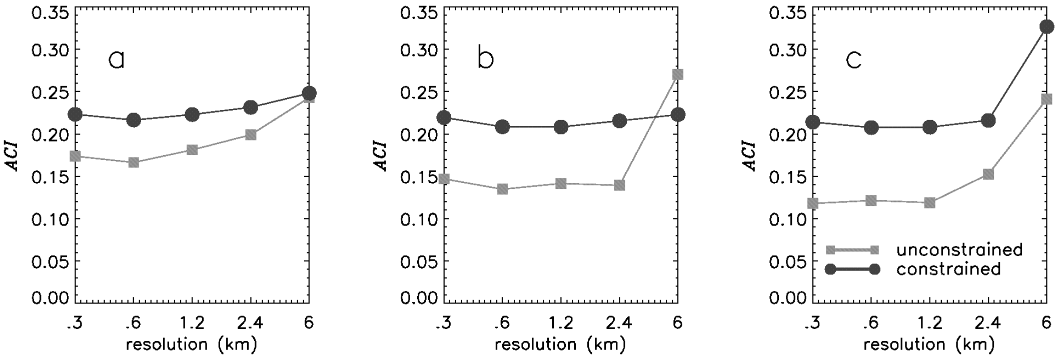

Fig. 12. Unconstrained and constrained ACI with change in level of aggregation for scenes **(a)**, **(b)**, and **(c)** in Fig. 5 (top row).

ACPD
11, 26741–26789, 2011

The scale problem in quantifying aerosol indirect effects

A. McComiskey and G. Feingold

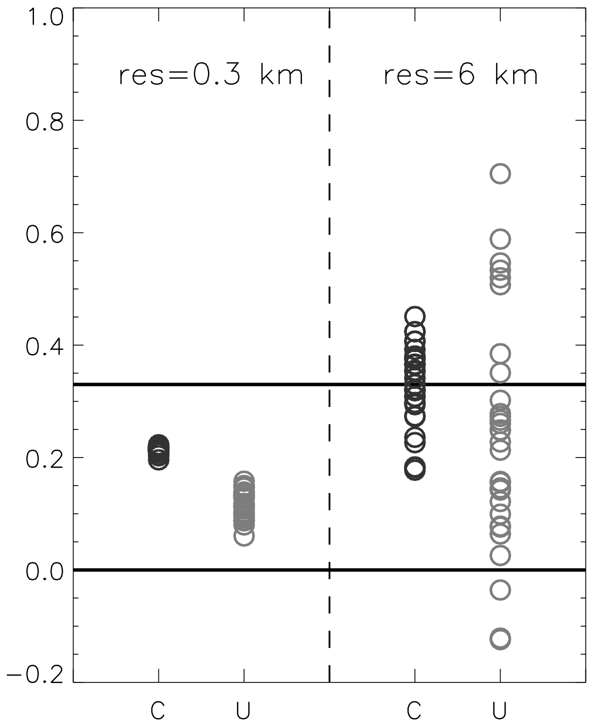

Fig. 13. Constrained (C) and unconstrained (U) ACI for the finest and coarsest resolutions of scene **(c)** from Fig. 5. Each set of constrained and unconstrained values consists of 30 data points. The horizontal lines at ACI = 0 and 0.33 mark the physical limit.

ACPD
11, 26741–26789, 2011